Academic Journal of Science and Technology
ISSN: 2771-3032 | Vol. 4, No. 3, 2022

Microstructure and Mechanical Properties of Homogenized AlxCrNbTiV (x=0.2,0.5,0.8) Refractory High Entropy Alloy

Haidong Chen[1, *]

[1] National-local Joint Engineering Laboratory of Intelligent Manufacturing Oriented Automobile Die & Mould, Tianjin University of Technology and Education, Tianjin 300222, China

[*] **Corresponding author**: CHEN Haidong (Email: 1454059277@qq.com)

Abstract: A new lightweight refractory high-entropy alloy $Al_xCrNbTiV$ (x=0.2; 0.5; 0.8) was prepared by vacuum arc melting method, and the changes in the microstructure and mechanical properties of the alloy after homogenization annealing at 1200°C for 24h were analyzed. The results shew that the homogenized $Al_xCrNbTiV$ alloy consists of a biphasic structure of BCC solid solution phase and C14 Laves phase, and the volume fraction of C14 Laves phase decreases with the increase of Al content and is not uniformly distributed. The alloy microhardness increased with increasing Al content, from 610HV for $Al_{0.2}CrNbTiV$ alloy to 673HV for $Al_{0.8}CrNbTiV$ alloy. Meanwhile, the yield strength decreased from 1705MPa to 1249MPa, the compressive strain decreased from 17.8% to 12.9%, and the brittleness increased with increasing Al content.

Keywords: Refractory high-entropy alloy, Annealing, Microstructure, Mechanical properties.

1. Introduction

The first batch of high entropy alloys (HEAs) composed of 3d transition group elements are usually composed of at least 4-5 elements, with a concentration close to the same molar ratio (5at.%~35at.%), which can have high strength, high hardness, wear resistance, corrosion resistance and other excellent properties. Recently, they have attracted extensive attention [1-5]. In order to expand the application of high entropy alloys in the field of high temperature, since 2010, people have proposed a new type of high entropy alloys with Mo, W, Nb, Hf, Ti, V, Zr and other refractory elements as the main components, called refractory high entropy alloys (RHEAs). The first batch of NbMoTaW and NbMoTaWV refractory high entropy alloys developed have a yield strength of 506MPa and 735MPa at 1600℃, which exceed the traditional nickel base superalloys and are expected to become high-temperature bearing structural materials [6]. However, the high density at room temperature limits its further application, which is 13.75 g/cm3 and 12.36 g/cm3 respectively, and does not have the lightweight property [7].

In this paper, the influence of different Al content on the phase composition, microstructure and mechanical properties of the alloy after homogenization annealing is further analyzed.

2. Experimental Methods

$Al_xCrNbTiV$ (x=0.2; 0.5; 0.8) refractory high entropy alloy button shaped ingots, hereinafter referred to as Al0.2, Al0.5 and Al0.8 respectively, were prepared by vacuum arc melting. The purity of raw materials powder is more than 99.9%. The nominal chemical composition is shown in Table 1. Alloy arc melting is carried out in a water-cooled copper furnace. Each sample is smelted at least five times to ensure chemical homogeneity. An ingot with a diameter of about 56mm and a height of 21mm is obtained. In order to prevent oxidation, the solid ingot is homogenized in argon atmosphere at 1200℃ for 24h and then cooled down to room temperature with a heating rate of 5℃/min.

The homogenized alloy shall be polished to a non marking mirror surface by mechanical polishing method, and then put into ethanol solution for ultrasonic cleaning for 30min before drying. Use 40Kv Cu-K α Radiation X-ray diffractometer (Bruker D8 ADVANCE A25, Germany) is used to detect the homogenized alloy at 2θ Crystal structure and phase composition within the range. Hitachi S-3400N scanning electron microscope (SEM) and energy dispersive spectrometer (EDS) were used to analyze the microstructure and element composition of the material. Use a Wolpert Wilson Instruments 401WVD to test the hardness of the polished surface under a load of 200g and a loading time of 15s, and measure at least 5 points of each sample to take its average hardness. Use Instron 5500R material testing machine to test 6×4×4mm³. The rectangular sample is subjected to isothermal compression test at room temperature, and the initial strain rate is $10^{-3}s^{-1}$， The experiment is stopped when the fracture or strain is 50%.

3. Results

3.1. Phase and structure of the $Al_xCrNbTiV$ alloys

The XRD patterns of the homogenized AlxCrNbTiV (x=0.2, 0.5, 0.8) alloys are shown in Fig. 1. The structure of AlxCrNbTiV alloys is composed of BCC phase and C14 Laves phase, which was already observed in an Al-Cr-Nb-Ti-V(-Zr) system HEAs. With an increase in Al content, the lattice parameter of bcc phase gradually decrease as the diffraction peaks of the bcc phase shift to higher degrees, whereas, the lattice constant of the C14 Laves get increased. The lattice constants for the solid solution could be obtained according to Bragg's law: $2d*\sin\theta=n\lambda$, where θ corresponds to the different diffraction peak. For bcc phase

$d = \frac{a}{\sqrt{h^2 + k^2 + l^2}}$, (h, k, l) represents the corresponding indices of crystal face. And the average BCC lattice constant could be calculated through the BCC diffraction peak, the calculated results show that the experimental lattice constant of the $Al_xCrNbTiV$ RHEAs decreases from 3.128Å for Al0.2 alloy to 3.123Å for Al0.8 alloy.

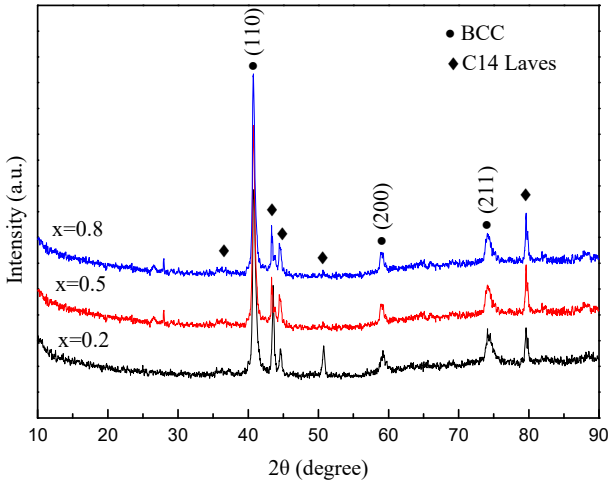

Figure 1. XRD patterns of the $Al_xCrNbTiV$ alloys

The microstructure of refractory $Al_xCrNbTiV$ alloys after homogenized at 1200℃ for 24h is shown in Figure 2. Apparently, all the $Al_xCrNbTiV$ alloys are composed of dark bcc matrix and the bright C14 hexagonal laves phase, which is in agreement with the XRD result. The SEM-EDS analysis exposed that the bcc matrix enriched with Ti, V, Nb and Al, and depletion of Cr, which is close to the alloy composition, although with slightly lower Cr content and higher Ti and Al content. And with the increase of Al content, some changes occurs to the chemical compositions of the bcc matrix, gradually increased Al content with continuous depletion of Nb and Ti, and almost unchanged concentration of Cr and V.

Large amount of second phase, that is C14 laves phase are formed in the bcc substrate, with volume fraction of 52%, 46.9% and 40.6% for Al0.2, Al0.5, Al0.8, respectively, measured from SEM, means that with the addition of Al, the precipitation of laves phase get decreased. One should note that the morphology of C14 laves phase are not the same for different alloy. For all $Al_xCrNbTiV$ alloys, the C14 laves phase precipitates as small and large particles at the same time. For Al0.2, the small particles homogeneously distributed in bcc matrix with irregular shape with the size about 1.64μm, while the large particles grows into almost rectangular particles with an average length and width of 7.8μm and 1μm, and the C14 laves phase with lager size is surrounded by fine particles, the distribution of the precipitations are relatively uniform. The C14 laves phase is mainly composed of Nb, Cr and Al, which can be defined as C14 $Nb(Cr, Al)_2$ type phase. And the EDS results show that no obvious change of the chemical composition is detected between the particles with different morphology for Al0.2 alloy. As the increase of Al content, the larger particles size increase sharply, the size difference for C14 laves phase become more obvious. For Al0.8, the coarsed particles still distribute as rectangular particles, but the particles size become much coarser, with average transversal and longitudinal sizes of 3.6μm and 11.6μm. And the finer particles still keep small grain size, on the order of ~3μm. One should also note that the distribution of the precipitations become not evenly with higher Al content, the relatively independent coarse-grain zone and fine-grain zone are even formed for Al0.8 alloy, although the crystal structure keep as C14 $Nb(Cr, Al)_2$ type laves phase. It could be concluded that with the increase of Al content, more Al segregates in C14 phase, and the size difference and inhomogeneous distribution of precipitated C14 phase within one alloy become more seriously, and all the C14 phase with different morphology is C14 $Nb(Cr, Al)_2$ type laves phase.

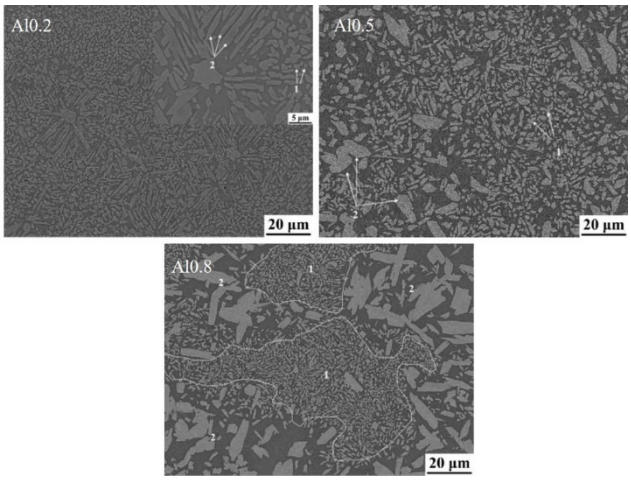

Figure 2. Microstructure of $Al_xCrNbTiV$ alloys

3.2. Properties of the $Al_xCrNbTiV$ alloys

3.2.1. Microhardness

Figure 3 shows the microhardness of the $Al_xCrNbTiV$ alloy system after homogenization at 1200℃ for 24h. With the increase of the content of Al, the hardness values of the $Al_xCrNbTiV$ alloy increase markedly. The hardness of the Al0.2 alloys is approximately 610HV, while 642HV and 673HV for Al0.5 and Al0.8 respectvely. The indentations of Al 0.8 alloy produces cracks emanating from the indent corners after hardness testing, proving high brittleness of this material. The high hardness value of $Al_xCrNbTiV$ after homogenization could be related to lattice distortion effect of alloy structure and slow diffusion effect on dynamics.

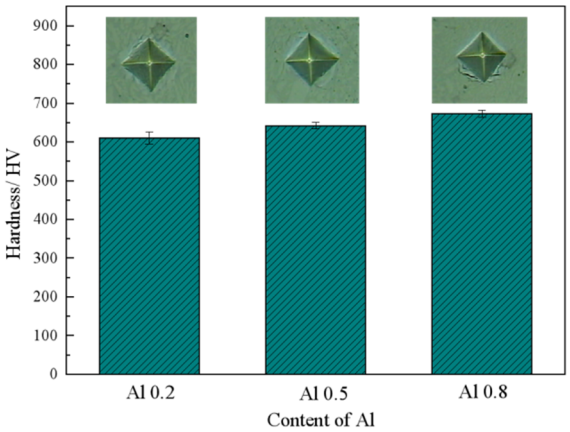

Figure 3. Microhardnesses of the $Al_xCrNbTiV$ alloy

3.2.2. Compression mechanical properties

Figure 4 shows the room temperature compressive engineering stress-strain curves for the $Al_xCrNbTiV$ alloys after homogenization with different Al contents. Compression

mechanical properties of the Al$_x$CrNbTiV alloys, namely yield strength σ_{YS}, fracture stress σ_P, and compression fracture strain ε, are shown in Table 1. The Al content had a pronounced effect on the compressive properties of the alloys. The studied alloys exhibit relatively high brittleness and fracture occurs in the elastic region of the stress-strain curves. With the increase of Al content, the fracture strength decreases remarkably as well as the strain. For Al0.2, the fracture stress is 1841.97 MPa with ε=17.75%, while for Al0.8, the fracture stress decrease to 1251.93 MPa with ε=12.92%.

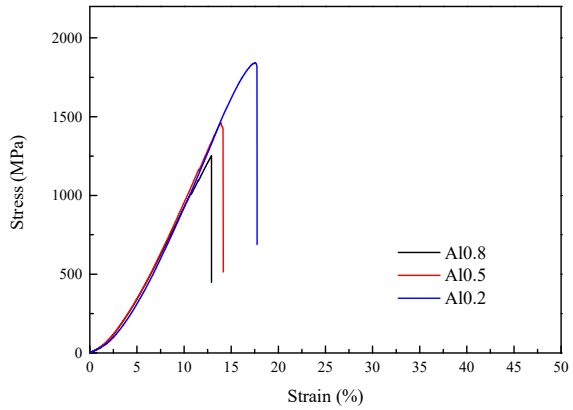

Figure 5. Compressive stress-strain curves of the Al$_x$CrNbTiV alloys at room temperature

Table 1. Room temperature compression mechanical properties of homogenized Al$_x$CrNbTiV alloys

Alloys	Fracture strength σ_b/MPa	Yield strength σ_s/MPa	Strain ε/%
Al0.2	1841.97	1705.02	17.75
Al0.5	1452.51	1460.27	14.14
Al0.8	1251.93	1249.65	12.92

3.2.3. Wear properties

After homogenization annealing at 1200℃ for 24h, the friction coefficient of Al0.2 alloy is the highest, which is 0.75. With the increase of Al element, the friction coefficient of Al0.5 and Al0.8 alloys is 0.73 and 0.71, respectively. The reduction of friction coefficient is closely related to the micro hardness of the alloy. Vickers hardness is the most important parameter for wear resistance. Combined with the micro hardness of alloys with different Al content in Figure 5, the results show that the friction coefficient decreases with the increase of hardness, which is consistent with the theoretical analysis, that is, the wear resistance is positively related to Vickers hardness. All alloy surfaces show deep and wide grooves along the horizontal friction and wear direction due to the grinding of Si_3N_4 ceramic balls. The volume loss decreases with the increase of Al content, and the wear volume loss is 0.021 mm³、0.019 mm³ and 0.016mm³。 After 20 min wear, the wear scar depth of Al0.2 alloy with the highest friction coefficient is greater than that of the other two component alloys, while the Al0.8 alloy with the lowest friction coefficient shows lower wear volume loss, wear depth and wear width are significantly smaller than those of the other component alloys, showing good wear resistance.

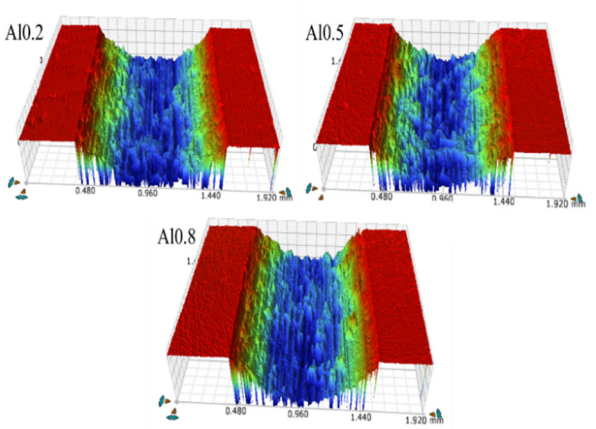

Figure 5. Surface Wear Morphology of Al$_x$CrNbTiV Alloy

4. Conclusion

In this paper, the changes of microstructure and mechanical properties of Al$_x$CrNbTiV (x=0.2; 0.5; 0.8) light refractory high entropy alloy after homogenization annealing at 1200℃ for 24h were studied. The following conclusions were obtained:

(1) Homogenized Al$_x$CrNbTiV alloy consists of BCC solid solution and C14 Laves phase structure. With the increase of Al content, the structure of C14 Laves phase becomes coarse and uneven, and the volume fraction decreases from 52% to 46.9%.

(2) With the increase of Al content, the microhardness of homogenized Al$_x$CrNbTiV alloy increases slowly from 610HV to 673HV.

(3) With the increase of Al content, the yield strength of homogenized Al$_x$CrNbTiV alloy decreases from 1705MPa to 1249MPa, and the compressive strain decreases from 17.8% to 12.9%.

References

[1] Yeh J W, Chen S K, Lin S J, et al. Nanostructured high-entropy alloys with multiple principal elements: novel alloy design concepts and outcomes[J]. Adv. Eng. Mater., 2004, 6: 299.

[2] Zhang Y, Zuo T T, Tang Z, et al. Microstructures and properties of high-entropy alloys[J]. Prog. Mater. Sci., 2014, 61: 1.

[3] Miracle D B, Senkov O N. A critical review of high entropy alloys and related concepts[J]. Acta Mater., 2017, 122: 448.

[4] Tsai K Y, Tsai M H, Yeh J W. Sluggish diffusion in Co-Cr-Fe-Mn-Ni high-entropy alloys[J]. Acta Mater., 2013, 61: 4887.

[5] Tang Z, Yuan T, Tsai C W, et al. Fatigue behavior of a wrought Al0.5CoCrCuFeNi two-phase high-entropy alloy[J]. Acta Mater., 2015, 99: 247.

[6] Senkov O N, Wilks G B, Scott J M, et al. Mechanical properties of Nb25Mo25Ta25W25 and V20Nb20Mo20Ta20W20 refractory high entropy alloys[J]. Intermetallics, 2011, 19: 698.

[7] Senkov O N, Wilks G B, Miracle D B, et al. Refractory high-entropy alloys[J]. Intermetallics, 2010, 18: 1758.